Препринти Інституту фізики конденсованих систем НАН України розповсюджуються серед наукових та інформаційних установ. Вони також доступні по електронній комп'ютерній мережі на WWW-сервері інституту за адресою http://www.icmp.lviv.ua/

The preprints of the Institute for Condensed Matter Physics of the National Academy of Sciences of Ukraine are distributed to scientific and informational institutions. They also are available by computer network from Institute's WWW server (http://www.icmp.lviv.ua/)

Дмитро Валерійович Портнягін

Чисельне моделювання розрядки літієвої батареї з мікропористим вуглецевим електродом

Роботу отримано 1 вересня 2006 р.

Затверджено до друку Вченою радою ІФКС НАН України

Рекомендовано до друку семінаром відділу теорії нерівноважних процесів

Виготовлено при ІФКС НАН України
© Усі права застережені

Національна академія наук України

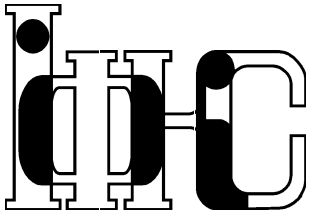

ІНСТИТУТ ФІЗИКИ КОНДЕНСОВАНИХ СИСТЕМ

ICMP–06–12E

Dmitry Portnyagin*

SIMULATION OF DISCHARGE OF LITHIUM BATTERY WITH MICROPOROUS CARBON ELECTRODE

*E-mail: port@icmp.lviv.ua

ЛЬВІВ

УДК: 541.13; 53.072; 53:681.3; 539.219.3; 538.931-405

PACS: 82.47.Aa, 82.45.Gj, 82.45.Fk, 82.45.-h, 82.20.Wt

Чисельне моделювання розрядки літієвої батареї з мікропористим вуглецевим електродом

Д.В. Портнягін

Анотація. Чисельно моделювалася розрядка літієвої батареї із вуглецевим мікропористим електродом в режимі заданого струму. Порівнювалися передбачення двох моделей: без електростатичного поля та з електростатичною взаємодією всередині частинок вуглецевого електрода. Спостерігалася певна розбіжність між ними.

Simulation of discharge of lithium battery with microporous carbon electrode

D.V. Portnyagin

Abstract. Discharge of lithium cell with microporous carbon electrode under galvanostatic control has been modelled. Predictions of the models without electric field and with electrostatic interaction inside the particles of carbon electrode have been compared. It has been observed a considerable difference between both.

Подається в Электрохимия
Submitted to Electrochemistry

© Інститут фізики конденсованих систем 2006
Institute for Condensed Matter Physics 2006

1. Introduction.

Rapid development in recent years in the market of mobile phones, laptop computers, other portable devices and electric vehicles evoke the demand for a high energy density portable power sources. In such batteries lithium often serves as a cathode material because of its low electronegativity. Porous materials are used for anode due to their large surface area associated with high energy storage. Mathematical simulation of charge/discarge processes allows to optimize the battery in order to obtain a higher performance. This can also help to analyze these processes to gain a deeper insight into the nature and courses of phenomena that occur during the discharge of these devices. Recently the simulation of the intercalation of lithium into the structure of porous electrode has been attracting the attention of several authors [3], [1], [5]. It is widely held that the main driving force at the operation of the battery is diffusion and that the transport of ions across the electrode is governed by Fick's second law. In the present paper we have made an improvement on this approach by taking into account electrostatic interaction between ions and with the distribution of charge in the bulk of porous electrode. Comparison of the predictions of the diffusive and the more realistic electrodynamic model testifies to that there is a certain discrepancy between them.

2. Basic considerations. Cylindrical particles.

We study the galvanostatic discharge of lithium battery. In our research we heavily rely upon the data from [1]. The battery consists of lithium foil, porous separator of thickness $L_s = 25\mu m$, porous carbon electrode of thickness $L_1 = 125\mu m$ made of either cylindrical or spherical particles of radius $R_s = 3,5\mu m$, and current collector. The battery is immersed in 1M solution of $LiClO_4$ in propylene carbonate.

The battery is discharged from its initial state with $U_0 = 0.91489V$ to $0.01V$ cutoff voltage at current densities $120.46A/m^2$ and $12.05A/m^2$.

During the discharge of the battery, lithium is dissolved into lithium ions from the negative electrode, migrates through the separator and finally intercalates into the carbon electrode. During the charge the reverse process takes place. We neglect the electrodes expansion and contraction. There exist two approaches for modelling lithium insertion into the particle, both of which lead to solving the diffusion equation in a particle. In the first approach the driving force is the gradient of concentration while the diffusion coefficient remains constant. However, it

has been reported that there is a strong dependence of the diffusion coefficient on concentration due to the lithium ion-lithium ion interactions inside the particle, which can not be ignored to obtain good agreement with experimental data. In the second approach Verbrugge and Koch [6] considered the gradient of the chemical potential of the inserted lithium ions as the driving force.

In the present section we consider cylindrical particles with the ratio of length to radius sufficiently large, for which the concentration of lithium inside the particle is a function only of radial distance, governed by the equation

$$\frac{\partial y}{\partial \tau} = \frac{1}{R}\frac{\partial}{\partial R}\left(Rf\frac{\partial y}{\partial R}\right) \tag{2.1}$$

$$y = y_0, \quad \text{at} \tau = 0, \forall R; \tag{2.2}$$

$$\frac{\partial y}{\partial R} = 0 \quad \text{at} R = 0, \forall \tau; \tag{2.3}$$

$$\frac{\partial y}{\partial R} = -\frac{j_n^+}{D_s}\frac{R_s}{C_{s,max}f} \quad \text{at} R = 1, \forall \tau; \tag{2.4}$$

where $\tau = tD_s/R_s^2$, $y = C_s/C_{s,max}$, $R = r/R_s$; are dimensionless variables. D_s is the diffusion coefficient in the solid phase, assumed to be constant, R_s is the radius of the particle, C_s is the concentration of lithium ions inside the particle, $C_{s,max}$ is the maximum concentration of lithium ions inside the particle, f is the activity factor dependant on the intercalation fraction and calculated by Verbrugge and Koch [6], j_n^+ is the flux of lithium ions at the surface of the particle. The initial value of y is equal to 0.01. The flux of lithium ions at the surface of the particle is equal to the electrochemical reaction rate per unit of surface area of the particle as given by a Butler-Volmer reaction rate expression

$$j_n^+ = K\left(C(1-y\big|_{R=1})\right)^{\beta-1}\left(y\big|_{R=1}\right)^{\beta} \times \left\{\exp\left[\frac{(1-\beta)F}{\Re T}(\eta - U)\right] - \exp\left[\frac{-\beta F}{\Re T}(\eta - U)\right]\right\},$$

where C is the concentration of the electrolyte, K is the reaction rate constant ($K = k_c^{1-\beta}k_a^{\beta}$), F is the Faraday constant, $\Re$ is universal gas constant, T is temperature, η is the potential between solid phase and electrolyte, and U represents the open-circuit cell potential with respect to a metallic lithium electrode which is evaluated at the surface of the particle where the electrochemical reaction takes place and which is given

by

$$U = U_s + \frac{\Re T}{F}\ln\left(\frac{1-y\big|_{R=1}}{y\big|_{R=1}}\right) - \sum_{s=2}^{7}\frac{\Omega_s}{F}s(y\big|_{R=1})^{s-1} \quad \text{for} \quad 0 < y|_{R=1} < 0.985, \tag{2.5}$$

where U_s is the standard cell potential with respect to a metallic lithium electrode, and Ω_s are the self-interaction energies. The material of which is made carbon electrode is not well-ordered, so the open-circuit potential does not exhibit plateaus or phase changes. We take the activity coefficient

$$f = 1 \tag{2.6}$$

for purely diffusive model, and

$$f = \left(1 + \frac{d\ln\gamma_+}{d\ln y}\right) = 1 + \sum_{s=2}^{7}\frac{\Omega_s}{\Re T}s(s-1)(y^{s-1} - y^s) \tag{2.7}$$

for chemical potential model (at low lithium concentrations f increases with increasing the lithium ion concentration due to repulsive effects, takes on its maximum at $y = 0.2$, and decreases with increasing the lithium ion concentration due to low ion mobility at higher concentrations). Our amendment to the aforementioned models consists in adding the current coursed by electric field to the righthand side of equation (2.1).

$$\frac{\partial y}{\partial t} = \frac{1}{R}\frac{\partial}{\partial R}\left(R\frac{D_s}{R_s^2}f\frac{\partial y}{\partial R}\right) - \frac{1}{FC_{max,s}}\text{div}(\sigma E), \tag{2.8}$$

where E is the electric field, σ the ionic conductivity given by Einstein relation

$$\sigma = yC_{max,s}N_aD_se^2/kT,$$

k is Boltzman constant, e is elementary charge, N_a is Avogadro number.

In the first approximation we assume that the current of positive ions through the surface of the particle is entirely due to the uniform distribution within the particle of negative charge, which carbon, being more electronegative, draws from lithium, and the distribution of charge caused by imposed external electric field. However, X-ray photoelectron spectroscopy (XPS) proved [4] that after insertion the lithium retains only a fraction of the positive charge $+\delta$, while the carbon takes a negative charge $-\delta$. Therefore to the distribution of charge in the bulk of the

particle we add the term associated with the nonuniform distribution of lithium ions. This results in

$$\mathrm{div}(E) = \frac{2}{R_s \sigma_{eff,1}} j_n^+ - \delta \frac{F C_{max,s}}{\varepsilon_0}(y_{avr} - y),$$

where $\sigma_{eff,1}$ is the effective conductivity of electrolyte in the carbon electrode, ε_0 is the dielectric constant, $y_{avr} = \int y dV/V = 2\int\limits_0^1 yRdR$ (or $= 3\int\limits_0^1 yR^2 dR$ for spherical particles) is the average concentration of ions in the particle, δ is the delocalization factor which equals 1 when we have naked lithium ions and negative charge, drawn from lithium, uniformly spread over carbon sites, and equals 0 when negative charge is maximally localized on lithium ions.

We shall refer to the insertion of lithium ions as a process given by the solution of (2.1)-(2.4) with f given by (2.6) the (DFM) model, and with f given by (2.7) - the (CPM) model. We shall call the diffusion process described by (2.8), (2.2)-(2.4) with f given by (2.6) the (DFME) model, and with f given by (2.7) - the (CPME) model.

The ionic current across the carbon electrode i_2 is equal to the external current through the battery i_{app} at the contact with separator, and is zero at current collector. Between these two values the current is assumed to be distributed according to the equation:

$$\frac{\partial i}{\partial x} = aF j_n^+,$$

where a is the interfacial area of particles per unit volume of porous electrode, calculated by

$$a = 0.03 \cdot 2(1-\epsilon_1)/Rs,$$

for the case of cylindrical particles, or by

$$a = 0.02 \cdot 3(1-\epsilon_1)/Rs$$

for spherical; ϵ_1 - porosity of carbon electrode. It appears quite obvious that after we have pressed and baked the carbon material, only a fraction of the particle's surface will be exposed to electrolyte, so we have introduced a suitable factor in the formula for the interfacial area. These factors are chosen such in order to match the experimental values of currents on cyclic voltammograms. The equation for the concentration

of the electrolyte in the solution phase of the carbon electrode is

$$\epsilon_k \frac{\partial C}{\partial t} = \nabla\left(\epsilon_k D_{eff,k} \nabla C\right) + a(1-t_+^0) j_n^+,$$

where $k = 1, s$ (1 corresponds to electrode, s to separator), t_+^0 is transfer number, $D_{eff,k} = \epsilon_k^{0.5} D$, D is the diffusion coefficient of electrolyte, $C_{initial} = 1000 \quad mol/m^3$. We impose on C the following boundary conditions: (i) that the flux of ions at lithium electrode is equal to the applied current through the cell

$$\epsilon_s D_{eff,s} \nabla C\big|_{x=0} = i_{app}/F,$$

(ii) that the flux of mass is continuous at the separator-electrode interface

$$\epsilon_s D_{eff,s} \nabla C\big|_{x=L_s-0} = \epsilon_1 D_{eff,1} \nabla C\big|_{x=L_s+0},$$

and (iii) that its's equal to zero at current collector

$$\epsilon_1 D_{eff,1} \nabla C\big|_{x=L_s+L_1} = 0.$$

The potential in the solution phase is

$$\nabla \phi_1 = -\frac{i_2}{\sigma_{eff,k}} + \frac{\Re T(1-t_+^0)}{FC} \nabla C,$$

where $\sigma_{eff,k}$, $k = \{1, s\}$ is the effective conductivity of electrolyte given in Table I.

The potential in the solid phase of the electrode is

$$\nabla \phi_2 = -\frac{(i_{app} - i_2)}{\sigma_{eff}},$$

where $\sigma_{eff} = \epsilon_1^{1.5}\sigma$ is the effective conductivity of electrode. The local surface overpotential is given by

$$\eta = \phi_1 - \phi_2.$$

The total voltage of the cell is related to η by

$$V_{total} = \eta\big|_{x=0} + (\phi_1 - \phi_2)_{kin} - \int\limits_{x=L_s}^{x=L_s+L_1} \frac{[i_{app} - i_2(x)]}{\sigma_{eff}},$$

Table I. Standard cell potential, interaction energies, model parameters for the carbon-lithium cella and physical constants.

Parameter	Value
U_0	$0.91489 \quad V$
U_s	$0.8170 \quad V$
Ω_2/F	$0.9926 \quad V$
Ω_3/F	$0.8981 \quad V$
Ω_4/F	$-5.630 \quad V$
Ω_5/F	$8.585 \quad V$
Ω_6/F	$-5.784 \quad V$
Ω_7/F	$1.468 \quad V$
$C_{s,max}$	$18,000 \quad mol/m^3$
β	0.5
K	$3.28 \times 10^{-6} \quad mol^{1/2}/m^{1/2}s$
K_{Li}	$4.1 \times 10^{-6} \quad mol^{1/2}/m^{1/2}s$
$C_{initial}$	$1000 \quad mol/m^3$
$T_{initial}$	$298 \quad K$
$y_{initial}$	0.01
D	$2.6 \times 10^{-10} \quad m^2/s$
D_s	$1.0 \times 10^{-14} \quad m^2/s$
t_+^0	0.2
$\sigma_{eff,k}$	$\epsilon_k^{1.5} C^{0.855}(0.00179\exp(-0.08(0.00083C-0.6616)^2 - 0.0010733C+0.855)) + 0.0001$
σ_{el}	$100 \quad S/m$
R_s	$3.5 \times 10^{-6} \quad m$
L_s	$25 \times 10^{-6} \quad m$
L_1	$125 \times 10^{-6} \quad m$
k	$1.381 \times 10^{-23} \quad J/K$
N_a	$6.022 \times 10^{23} \quad mol^{-1}$
$\Re$	$8.314 \quad J/(mol \cdot K)$
F	$96,487 \quad C/mol$
ε_0	$8.854 \times 10^{-12} \quad C^2/(N \cdot m^2)$
e	$1.9 \times 10^{-19} \quad C$
δ	10^{-9}
ϵ_1	0.35
ϵ_s	0.55

where $(\phi_1 - \phi_2)_{kin}$ is given by kinetic expression

$$i_{app} = FK_{Li}C^{0.5}(\exp((0.5F/(\Re T))(\phi_1 - \phi_2)) - \\ - \exp(-(0.5F/(\Re T))(\phi_1 - \phi_2)))$$

with K_{Li} - the reaction rate constant at the lithium electrode.

The utilization of the cell u is defined by

$$u = (2/L_1) \int_{x=L_s}^{x=L_s+L_1} dx \int_{R=0}^{R=1} yRdR,$$

for cylindrical particles, or by

$$u = (3/L_1) \int_{x=L_s}^{x=L_s+L_1} dx \int_{R=0}^{R=1} yR^2dR$$

for spherical ones.

All the parameters of the cell are evaluated at $T_{initial} = 298K$ for the reasons explained in [2]. The values of the standard cell potential, the self-interaction energies, and the kinetic parameters are given in Table I.

To determine the temperature of the cell we make the assumptions that the distribution of temperature throughout the cell is uniform at a given instant in time and the enthalpy of mixing and phase-change terms are neglected. With these assumptions the temperature is calculated according to the equation

$$\varrho C_p \frac{\partial T}{\partial t} = a_1 a_2 h(T_{amb} - T) + a_1 i_{app}\left(U - V_{total} - T\frac{dU}{dT}\right),$$

where ϱ is the density of the cell, C_p is the heat capacity the cell, calculated as the average of the components of the cell, a_1 is the geometric electrode surface area per volume of the cell, a_2 is the ratio of external cell surface area to geometric electrode surface area, T_{amb} is the ambient temperature, and h is the heat transfer coefficient. The entropy term $\frac{dU}{dT}$ is obtained by taking the derivative of (2.5) with respect to T:

$$\frac{dU}{dT} = \frac{\Re}{F}\ln\left(\frac{1-y|_{R=1}}{y|_{R=1}}\right) \quad \text{for} \quad 0 < y|_{R=1} < 0.985.$$

The mean cell density and heat capacity are calculated by formulas:

$$\varrho = (\varrho_s(1-\epsilon_s)L_s + \varrho_1(1-\epsilon_1)L_1 + \varrho_{c,1}L_{c,1} + \\ +\varrho_{Li}L_{Li})\,/(L_1 + L_s + L_{c,1} + L_{Li}),$$

$$C_p = (C_{p,PC}\varrho_{PC}(L_1\epsilon_1 + L_s\epsilon_s) + C_{p,1}\varrho_1 L_1 + C_{p,Cu}\varrho_{c,1}L_{c,1} + \\ +C_{p,Li}\varrho_{Li}L_{Li})\,/(\varrho_{PC}(L_1\epsilon_1 + L_s\epsilon_s) + \varrho_1 L_1 + \varrho_{c,1}L_{c,1} + \varrho_{Li}L_{Li}),$$

where ϱ_s, $\varrho_{c,1}$, ϱ_{Li}, ϱ_{PC}, and ϱ_1 are, respectively, the densities of separator, current collector, lithium, propylene carbonate and carbon electrode, the latter defined for $y = 1$; $L_{c,1}$ and L_{Li} are the thicknesses of current collector and lithium electrode; $C_{p,PC}$, $C_{p,1}$, $C_{p,Cu}$, and $C_{p,Li}$ are the heat capacities of propylene carbonate, carbon electrode, current collector, and lithium. Heat parameters of the cell are given in Table II.

Table II. Heat parameters of the cell.

Parameter	Value
T_{amb}	$298 \quad K$
L_{Li} (for $y = 0.01$)	$4.1 \times 10^{-5} \quad m$
$L_{c,1}$	$9 \times 10^{-6} \quad m$
a_1	$5000 \quad m^{-1}$
a_2	0.084
h	$5 \quad W/(m^2 \cdot K)$
ϱ_s	$950 \quad kg/m^3$
ϱ_1	$2220 \quad kg/m^3$
$\varrho_{c,1}$	$8930 \quad kg/m^3$
ϱ_{Li}	$534 \quad kg/m^3$
ϱ_{PC}	$1200 \quad kg/m^3$
$C_{p,PC}$	$720 \quad J/(kg \cdot K)$
$C_{p,1}$	$8.875 + 0.378T \quad J/(kg \cdot K)$
$C_{p,Cu}$	$1.4 \times 10^{-6}T^3 - 1.6 \times 10^{-3}T^2 + \\ +0.987T + 225 \quad J/(kg \cdot K)$
$C_{p,Li}$	$3.72T + 2423 \quad J/(kg \cdot K)$

The corresponding set of equations from Table III has been solved numerically.

One can see from Figures 1-3 that the graphs of the models in which we take into account electrostatic interaction lie, in general, above purely diffusive or chemical potential ones and the cell runs for longer time, as is seen from Table IV, thus resulting in a larger capacity of the cell. This is due to the fact that the presence of a negative charge distributed inside the particle promotes the insertion of lithium ions into the carbon particles, thus making its contribution to the total current through the battery. Thus, in the case of the presence of electrical charge the current due solely to diffusion is smaller. Now it is easily seen from the Butler-Volmer expression that this results in a smaller drop in voltage at a given instant in time. At the beginning of each process of discharge the graphs of the model with electric field lie closer to those of models without electrostatic interaction than at the final stages of discharge, because the profiles of concentration become more steep with time, as Figure 13 indicates, which results in a larger contribution to current due to electrostatic interaction. Comparison of Figures 2-3 shows that the relative difference between electrodynamic and non-electrodynamic models becomes more significant as the discharge current density increases. It looks like the electric field has its stable contribution to current which is the more transparent, the larger is the total current. In the case of a variable diffusion coefficient the graph of the model with electric field, as Figures 1, 2 indicate, is closer to that of chemical potential model than in the case of purely diffusive model, because the lithium ion - lithium ion interactions governed by the activity coefficient makes the term proportional to ∇y in $\mathrm{div}\sigma E$ in the diffusion equation not so significant due to more sloping concentration profile, caused by more uniform spreading of lithium ions inside the particle due to non-electrostatic interactions between ions.

The cell voltage being larger for a given utilization value, the temperature graphs in electrodynamic case lie above the non-electrodynamic ones, as Figures 7-9 show. Since the drop in voltage is smaller at each given instant in time in electrodynamic case for the reasons explained above, the cell runs for a longer period of time generating, thus, more ohmic heat. For the above-explained reasons the graphs of electrodynamic and non-electrodynamic cases are closer to each other in the case of larger discharge currents.

Table III. System of model equations and boundary conditions.

Region	Value	Equation or boundary condition
$x = 0$	y	$y = 0$
	C	$\epsilon_s D_{eff,s} \nabla C = i_{app}/F$
	i_2	$i_2 = i_{app}$
$0 < x < L_s$	y	$y = 0$
	C	$\epsilon_s \dfrac{\partial C}{\partial t} = \nabla \left(\epsilon_s D_{eff,s} \nabla C \right)$
	i_2	$i_2 = i_{app}$
	η	$\nabla \eta = \dfrac{i_2}{\sigma_{eff,s}} - \dfrac{\Re T (1 - t_+^0)}{FC} \nabla C$
$x = L_s$	C	$\epsilon_s D_{eff,s} \nabla C \big\vert_{L_s - 0} = \epsilon_1 D_{eff,1} \nabla C \big\vert_{L_s + 0}$
$L_s < x < L_s + L_1$	y	For cylindrical particles (2.1) with (2.2)-(2.4), or (2.8) with (2.2)-(2.4). For spherical particles (3.1) with (2.2)-(2.4), or (3.2) with (2.2)-(2.4).
	C	$\epsilon_1 \dfrac{\partial C}{\partial t} = \nabla \left(\epsilon_1 D_{eff,1} \nabla C \right) + a(1 - t_+^0) j_n^+$
	i_2	$\nabla i_2 = a F j_n^+$
	η	$\nabla \eta = \dfrac{-i_{app}}{\sigma_{eff}} + i_2 \left(\dfrac{1}{\sigma_{eff}} + \dfrac{1}{\sigma_{eff,1}} \right) - \dfrac{\Re T (1 - t_+^0)}{FC} \nabla C$
$x = L_s + L_1$	C	$\epsilon_1 D_{eff,1} \nabla C = 0$
	i_2	$i_2 = 0$

Table IV. Discharge times.

Model and discharge rate	Time to discharge
DFM, cylindrical, $i_{app} = 12.05 A/m^2$	231 s
DFME, cylindrical, $i_{app} = 12.05 A/m^2$	1514 s
DFM, spherical, $i_{app} = 12.05 A/m^2$	201 s
DFME, spherical, $i_{app} = 12.05 A/m^2$	683 s
CPM, cylindrical, $i_{app} = 12.05 A/m^2$	356 s
CPME, cylindrical, $i_{app} = 12.05 A/m^2$	548 s
CPM, cylindrical, $i_{app} = 120.46 A/m^2$	7.2 s
CPME, cylindrical, $i_{app} = 120.46 A/m^2$	35.5 s
CPM, spherical, $i_{app} = 12.05 A/m^2$	245 s
CPME, spherical, $i_{app} = 12.05 A/m^2$	425 s
CPM, spherical, $i_{app} = 120.46 A/m^2$	6.8 s
CPME, spherical, $i_{app} = 120.46 A/m^2$	7.2 s

3. Spherical particles.

For spherical particles equations (2.1) and (2.8) are replaced by

$$\frac{\partial y}{\partial \tau} = \frac{1}{R^2} \frac{\partial}{\partial R} \left(R^2 f \frac{\partial y}{\partial R} \right) \tag{3.1}$$

$$\frac{\partial y}{\partial t} = \frac{1}{R^2} \frac{\partial}{\partial R} \left(R^2 \frac{D_s}{R_s^2} f \frac{\partial y}{\partial R} \right) - \frac{1}{FC_{max,s}} \mathrm{div}(\sigma E), \tag{3.2}$$

$$\mathrm{div}(E) = \frac{3}{R_s \sigma_{eff,1}} j_n^+ - \delta \frac{FC_{max,s}}{\varepsilon_0} (y_{avr} - y).$$

The corresponding set of equations from Table III has been solved numerically.

In the same way as for cylindrical particles, Figures 4-6 indicate that the presence of a negative charge distributed inside the particle promotes the insertion of lithium ions into the carbon particles, which results in a smaller drop in voltage at a given instant in time, which, in turn, leads to larger values of cell capacity and to cell running for longer period of time. At the beginning of discharge the graphs of the model with electric field lie closer to those of models without field than at the end, due to steeper concentration profiles. The relative difference between electrodynamic and non-electrodynamic models is more significant as the discharge current density increases. In the case of a variable diffusion coefficient the graph of the model with electric field, as Figures 4, 5

indicate, is closer to that of chemical potential model than in the case of purely diffusive model.

The temperature graphs in electrodynamic case lie above the non-electrodynamic ones, as Figures 10-12 show. In electrodynamic case the cell runs for a longer period of time generating more ohmic heat. The graphs of electrodynamic and non-electrodynamic cases are closer to each other in the case of larger discharge currents.

Comparison of discharge graphs for spherical (Figures 4-6 and 10-12) and for cylindrical particles (Figures 1-3 and 7-9) testify that the influence of electrostatic field is more significant in the case of cylindrical particles because in that case the charge that produces this field occupies larger part of a space.

4. Conclusions.

We have made a simulation of the discharge of lithium cell with microporous carbon electrode under galvanostatic control. We have compared the predictions of the models in which electric field is not considered (CPM, DFM) and the ones in which electrostatic interaction of lithium ions between each other and with the distribution of charge in the bulk of carbon electrode is taken into account (CPME, DFME). We have observed that there is a considerable difference between the results predicted by both models. The models without electrostatic interaction underpredict the capacity of the cell. The form of the particles has some impact on the predictions of both models: in case of cylindrical particles the influence of electrodynamics is larger. In the case of a constant and variable diffusion coefficient the electrodynamic model allows the cell to run for longer period of time. The most adequate from the viewpoint of agreement with experiment proved to be the electrodynamic model with constant diffusion coefficient for cylindrical particles. This could make us think that the interactions between ions in the activity factor may be reduced solely to electrostatic interaction. This could also lead to conclusion that even in the case of spherical particles the structure of carbon electrode possesses cylindrical symmetry, i. e. the particles coagulate into fibers. The results indicate that the electrostatic interactions does matter, that the kinetic parameters obtained with the purely diffusive (DFM) or chemical potential model (CPM) may not represent the real kinetics of the system, and that the cell should be modelled using electrodynamic approach to get more adequate results.

References

1. G. G. Botte and R. E. White, J. Electrochem. Soc. **148** ((1) 2001), A54–A66.
2. G. G. Botte, B. A. Johnson, and R. E. White, J. Electrochem. Soc. **146** (1999), 914.
3. I. O. Polyakov, V. K. Dugaev, Z. D. Kovalyuk, and V. I. Litvinov, Russian Journal of Electrochemistry **Vol. 33, No. 1** (1997), 21Ц25.
4. R. Kanno, Y. Kawamoto, Y. Takeda, S. Ohashi, N. Imanishi, and O. Yamamoto, J. Electrochem. Soc. **139** (1992), 3397.
5. S.-I. Lee, Y.-S. Kim, H.-S. Chun, Electrochim. Acta **47** (2002), 1055–1067.
6. M. W. Verbrugge and B. J. Koch, J. Electrochem. Soc. **143** (1996), 600.

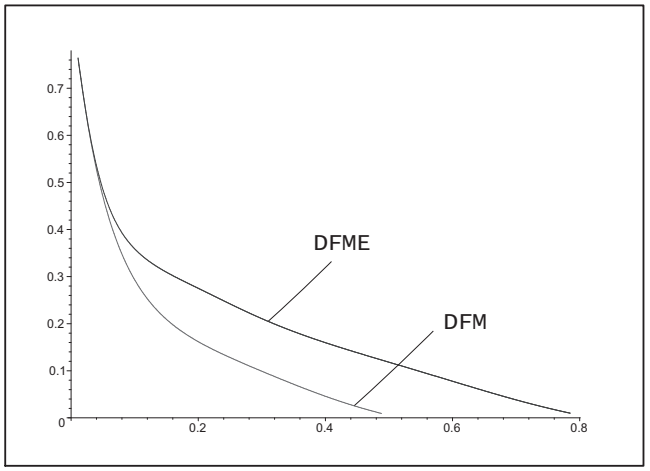

Figure 1. Cell voltage (V) vs. utilization at discharge rate 12.05 A/m^2 for cylindrical particles for purely diffusive model with (DFME) and without electric field (DFM).

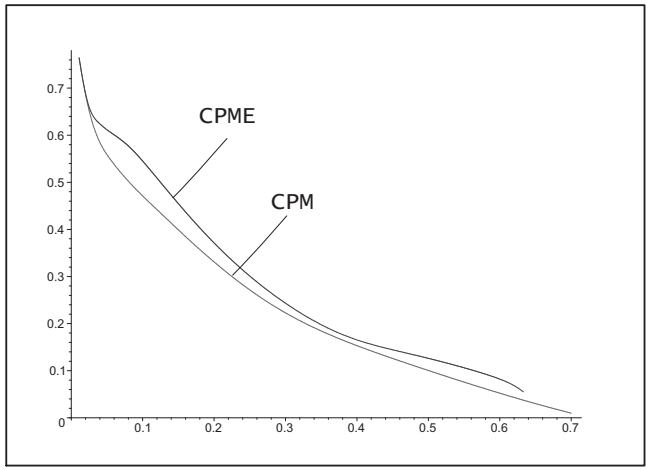

Figure 2. Cell voltage (V) vs. utilization at discharge rate 12.05 A/m^2 for cylindrical particles for chemical potential model with (CPME) and without electric field (CPM).

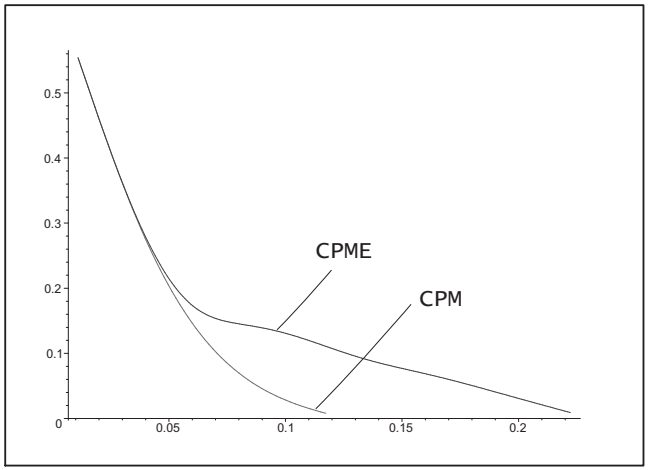

Figure 3. Cell voltage (V) vs. utilization at discharge rate 120.46 A/m^2 for cylindrical particles for chemical potential model with (CPME) and without electric field (CPM).

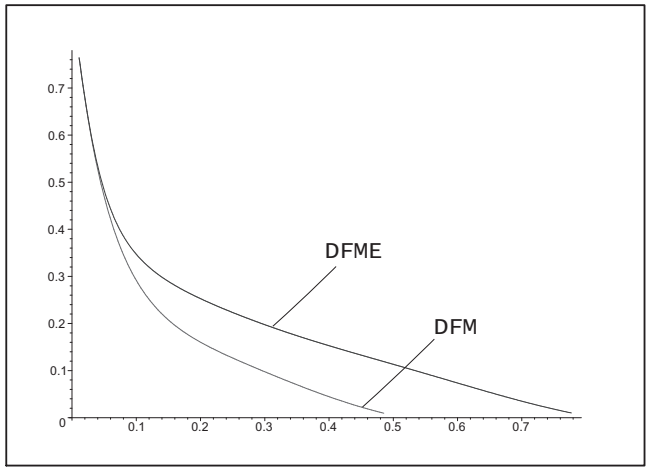

Figure 4. Cell voltage (V) vs. utilization at discharge rate 12.05 A/m^2 for spherical particles for purely diffusive model with (DFME) and without electric field (DFM).

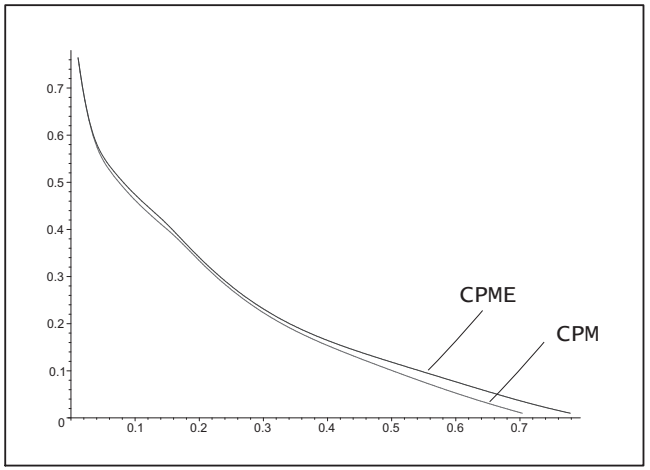

Figure 5. Cell voltage (V) vs. utilization at discharge rate 12.05 A/m^2 for spherical particles for chemical potential model with (CPME) and without electric field (CPM).

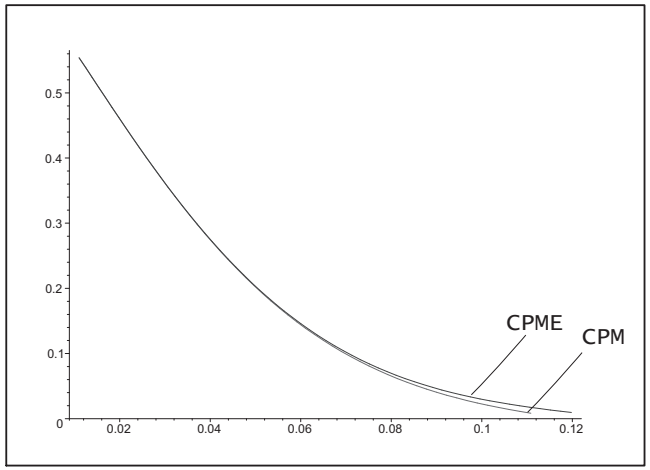

Figure 6. Cell voltage (V) vs. utilization at discharge rate 120.46 A/m^2 for spherical particles for chemical potential model with (CPME) and without electric field (CPM).

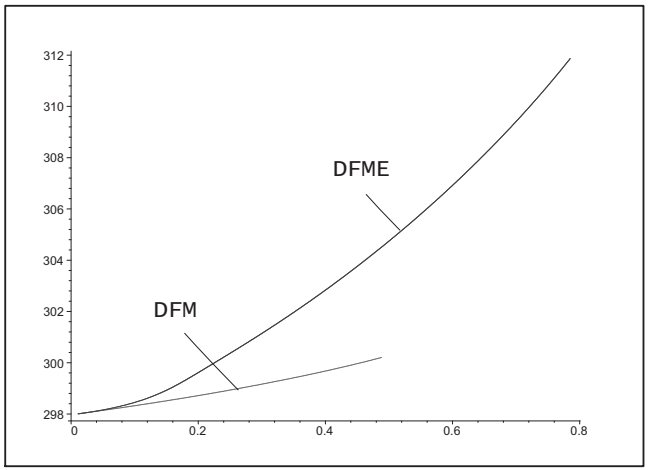

Figure 7. Temperature of the cell (K) vs. utilization at discharge rate 12.05 A/m^2 for cylindrical particles for purely diffusive model with (DFME) and without electric field (DFM).

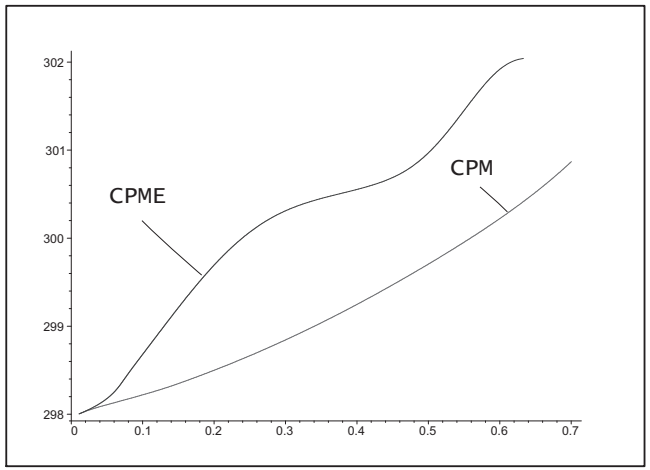

Figure 8. Temperature of the cell (K) vs. utilization at discharge rate 12.05 A/m^2 for cylindrical particles for chemical potential model with (CPME) and without electric field (CPM).

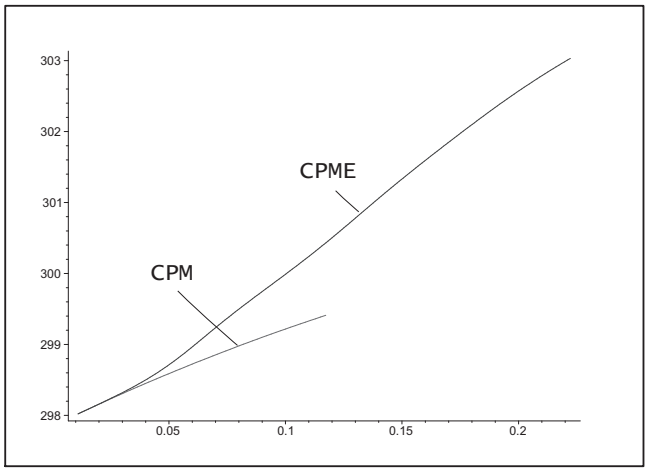

Figure 9. Temperature of the cell (K) vs. utilization at discharge rate 120.46 A/m^2 for cylindrical particles for chemical potential model with (CPME) and without electric field (CPM).

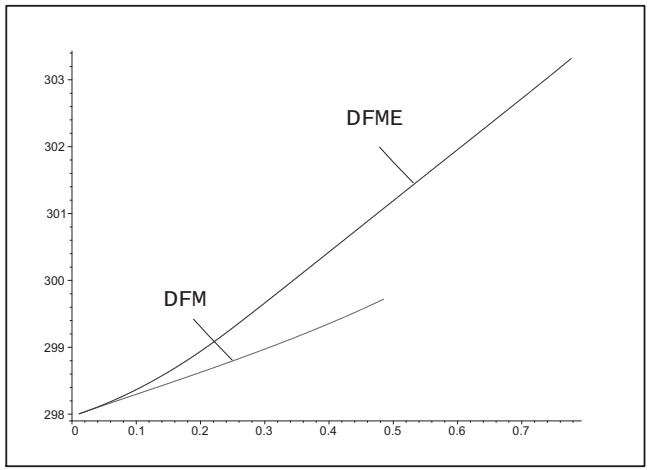

Figure 10. Temperature of the cell (K) vs. utilization at discharge rate 12.05 A/m^2 for spherical particles for purely diffusive model with (DFME) and without electric field (DFM).

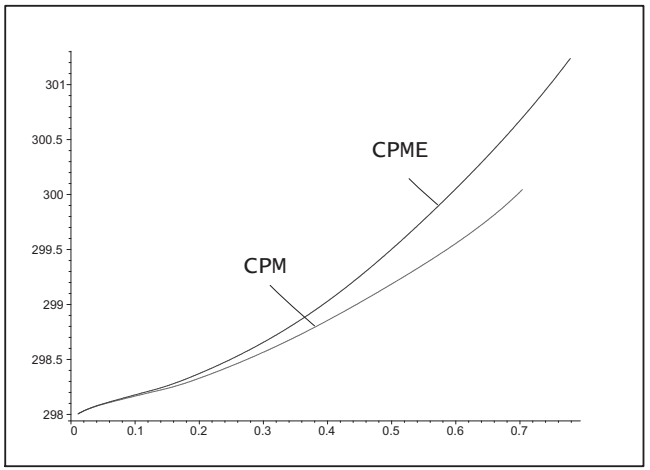

Figure 11. Temperature of the cell (K) vs. utilization at discharge rate 12.05 A/m^2 for spherical particles for chemical potential model with (CPME) and without electric field (CPM).

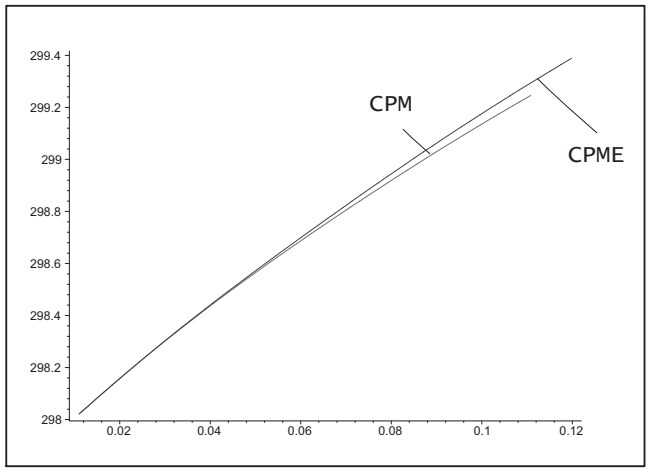

Figure 12. Temperature of the cell (K) vs. utilization at discharge rate 120.46 A/m^2 for spherical particles for chemical potential model with (CPME) and without electric field (CPM).

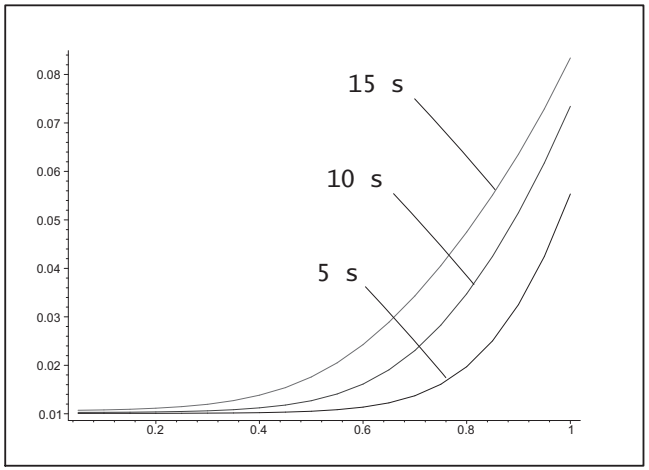

Figure 13. Dimensionless concentration vs. dimensionless radial distance for cylindrical particles located at distance $L_1/2$ from current collector, for chemical potential model with electric field (CPME) at 5, 10 and 15 seconds of discharge.